

# Modeling of terrain effect in magnetotelluric data from Garhwal Himalaya Region

Suman Saini<sup>1\*</sup>, Deepak Kumar Tyagi<sup>2</sup>, Sushil kumar<sup>3</sup>, Rajeev Sehrawat<sup>1\*\*</sup>

<sup>1</sup>Department of Physics, M. M. Engineering College, Maharishi Markandeshwar (Deemed to be) University, Mullana-Ambala, Haryana, India 133207

Corresponding Author- Rajeev Sehrawat<sup>1\*\*</sup>

\*\*Email: [rajeev.sehrawat@mmumullana.org](mailto:rajeev.sehrawat@mmumullana.org)

\*Email: [sumanabcd12@gmail.com](mailto:sumanabcd12@gmail.com)

<sup>2</sup>Department of Physics, Krishnan College of Science and IT, M.J.P. Rohilkhand University, Bijnor, Uttar Pradesh, India-246701

<sup>3</sup>Department of Geophysics, Kurukshetra University, Kurukshetra, India-136119

## ABSTRACT

Magnetotelluric methods (MT) are passive geophysical techniques based on time variations of the geoelectric and geomagnetic field in order to measure the electrical resistivity of surface layer. It is most effective geophysical techniques to study the deep structure of the Earth's crust, particularly in steep terrain like the Garhwal Himalaya region. The MT responses are distorted as a result of the undulated/rugged terrain. Such responses, if not corrected, can lead to a misinterpretation of MT data for the geoelectrical structures. In this study, two different correction procedures were used to compute the topography distortion for the synthetic model of Garhwal Himalaya region from Roorkee to Gangotri section. A finite difference algorithm was used to compute MT responses (apparent resistivity and phase) for the irregular terrain. The accuracy of the terrain correction procedures was checked on results published in the literature on different topography models at various periods. The relative errors between two terrain correction procedures were calculated with respect to flat earth and were very less or almost zero for most of the sites along the Roorkee to Gangotri profile except at the foothill where the error was high at lower periods. The similar topography response, terrain corrected

26 responses TCR1 and TCR2 responses concluded that there is no need for topography correction along  
27 Roorkee-Gangotri Profile because the slope angle is less than one degree.

28 **Keywords:** Magnetotelluric, Topography correction procedures, Himalaya region

## 29 1. INTRODUCTION

30 The magnetotelluric (MT) method was first explored by Tikhonov (1950) and Cagniard (1953) and  
31 was used to analyse the time-varying measured components of earth's natural time-varying electric  
32 and magnetic fields to determine the shallow layers of the Earth. MT technique has been successfully  
33 used to explore a variety of earth resources, including oil, gas, mineral, and geothermal energy (Zhang  
34 et al., 2014; Patro et al., 2017; Mohan et al., 2017). The MT method is effective for analysing deep  
35 crystal structures in challenging undulating terrains, such as the Himalayan region as compared to the  
36 seismic method (Tyagi , 2007; Israil et al., 2008, 2016; Pavan Kumar et al., 2014; Patro and  
37 Harinarayana, 2009; Kumar et al., 2018, 2022; Xiong-Bin, 2020; Dharmendra Kumar et al., 2021;  
38 Konda et al., 2023). Topography affects both the electric field and magnetic field components due to  
39 undulating topographical features like hills and valleys, which distort the current lines (Wannamaker  
40 et al., 1986; Michel Choutraus et al., 1988; Changhong et al., 2018; Kumar et al., 2018, 2022).  
41 Therefore, the MT response functions impedance and apparent resistivity get distorted when the MT  
42 sites are on or near the top of the hill or close to the valley.

43 Analytical and numerical techniques have been used to measure the topography distortion effect from  
44 MT data. Analytical techniques based on conformal mapping were used by Thayer (1975),  
45 Harinarayana and Sarma (1982). The 2D numerical techniques have been used for different type  
46 terrain geometries to remove topography effects from the data. The analogue, analytic, and numerical  
47 solution methods were used to study the analogue model (Wescott and Hessler, 1962; Faradzhev et al.,

48 1972). Various two-dimensional (2D) numerical techniques have been used for the numerical  
49 treatment of the topographic effects like networking analogy (Ku et al., 1973; NgCo, 1980) and  
50 Rayleigh scattering numerical modeling techniques (Reddig and Jiracek, 1984; Jiracek et al., 1989),  
51 finite element method (Wannamaker Stodt and Rijo, 1986; Frankle et al., 2007) and finite difference  
52 method (Josef Pek and Tomas Verner, 1996; Yutaka Sasaki, 2003 and Tyagi et al., 2007). The  
53 distortions in MT data due to topography and near-surface inhomogeneities have been observed by  
54 many researchers (Michel Choutraus et al., 1988; Jiracek, 1990; Vozoff, 1991). The distortion tensor  
55 stripping-off technique has been used to reduce the topographic effect and to remove the distortion  
56 due to the near-surface heterogeneity (Larsen, 1971). The analogue, analytic, and numerical solution  
57 methods were used to study the analogue model (Wescott and Hessler, 1962; Faradzhev et al.,  
58 1972). Various two-dimensional (2D) numerical techniques have been used for the numerical  
59 treatment of the topographic effects like networking analogy (Ku et al., 1973; NgCo, 1980) and  
60 Rayleigh scattering numerical modeling techniques (Jiracek Reddig and Kojima, 1989) and finite  
61 element method (Wannamaker Stodt and Rijo, 1986; Frankle et al., 2007). In 2D, the topography  
62 effect is galvanic in Transverse Magnetic (TM) mode and inductive in Transverse Electric (TE) mode,  
63 hence more distortion in TM mode than TE mode (Gurer and Ilikisik, 1997; Kumar et al., 2014;  
64 Kumar et al., 2018, 22).

65 In this study, modified 2D forward and inversion modeling code EM2INV (Rastogi, 1997) based on  
66 the finite difference method were used to compute MT forward modeling responses over flat earth and  
67 topographic surface. Two different terrain correction procedures have been used in this study: first  
68 correction procedure was adopted from Chouteau and Bouchard (1988) and the second was adopted  
69 from Nam et al., (2008) to compute the topography distortion for the synthetic model of

70 GarhwalHimalayan region (Roorkee-Gangotri section). The results of both terrain correction  
71 procedures have been compared with the model used by Chouteau and Bouchard (1988).

## 72 **2. METHODOLOGY**

73 The topography correction to the MT data has been applied by two different techniques. The first  
74 technique was introduced by Chouteau and Bouchard (1988) to estimate the distortion tensor and  
75 correction of MT data before inversion of MT data. In the second approach, the distortion tensor  
76 stripping-off technique was used to remove the distortion from the MT data (Larsen, 1977 and Nam et  
77 al., 2008). Two correction procedures, first adopted by Chouteau and Bouchard (1988) and second by  
78 Nam et al., (2008), were used to correct the MT data.

### 79 **2.1 Terrain correction procedure 1 (TCP1):-**

80 The computational algorithm for 2D forward modeling has been used to account for irregular terrain.  
81 The distortion tensor for the topographic effect was calculated using the technique adopted by  
82 Chouteau and Bouchard (1988). Based on the assumption that the topography distorted subsurface  
83 field can be approximated by multiplying the distortion tensor by the subsurface field for a flat earth  
84 given by:

$$85 \quad \widetilde{E}_D = D\widetilde{E}_N \quad (1)$$

86 where  $\widetilde{E}_D$  and  $\widetilde{E}_N$  are the distorted and normal electric field matrices with elements  $E(f,r)_D$  and  
87  $E(f,r)_N$  respectively.  $\widetilde{D}$  is the distortion tensor with elements  $D(f,r)$ , where  $f$  is frequency and  $r$  is  
88 the measuring site position. In case of 2D problem in TM mode and x-axis is the direction of strike,  
89 equation (1) can be written as

$$90 \quad E_{xD}(f,r) = D_{XX}(f,r)E_{xN}(f,r) \quad (2)$$

91 The impedance tensor can be calculated by dividing equation (2) by the magnetic field  $H_Y$ .

$$92 \quad Z_D(f, x) = D(f, x)Z_N(f, x) \quad (3)$$

93 where  $Z_N(f, x)$  and  $Z_D(f, x)$  are respectively the normal (flat earth) impedance and distortion  
94 impedance. The complex coefficients  $D(f, x)$  are distortion coefficients that should just reflect  
95 topography effect. The distortion coefficients are calculated by normalizing the impedances  $Z_t(f, x)$   
96 computed over topographic model above a homogeneous medium with the half-space impedance.  
97 Thus, the corrected impedance over flat earth can be calculated by taking the following ratio of the  
98 observed impedances,  $Z_D(f, x)$ , over irregular topography to the distortion coefficients  $D(f, x)$ :

$$99 \quad Z_C(f, x) = Z_D(f, x)/D(f, x) \quad (4)$$

100 where  $Z_C(f, x)$  is terrain-corrected impedance.

## 101 **2.2 Terrain correction procedure 2 (TCP2) :-**

102 In this correction procedure, the MT data was corrected using the technique adopted by Nam et al.,  
103 (2008). Larsen (1977) introduced the distortion tensor stripping-off technique, in which the  
104 undistorted impedance tensor can be calculated using a linear relationship between the distorted and  
105 undistorted impedance tensor, and topography distorted MT data can be corrected by computing the  
106 distortion tensor. The undistorted impedance tensor is linearly related to the distorted impedance  
107 tensor as:

$$108 \quad Z^D = D^Z \cdot Z^U \quad (5)$$

109 where  $Z^D$  is the distortion impedance tensor,  $D^Z$  is distortion tensor and  $Z^U$  is the undistorted  
110 impedance tensor respectively. The distortion tensor can be calculated from the relation between the

111 impedance tensor for a homogeneous medium with topography earth surface ( $Z^t$ ), and that with the  
 112 flat earth surface ( $Z^h$ ) as

$$113 \quad Z^t = D^Z \cdot Z^h \quad (6)$$

114 In case of 2D,  $Z_{xx}^h = Z_{yy}^h = (0, 0)$  and  $Z_{xy}^h \neq -Z_{yx}^h$ , the inhomogeneous earth distortion tensor,  
 115 equations (5) and (6) can be rewritten in matrix form as

$$116 \quad \begin{bmatrix} 0 & Z_{xy}^D \\ Z_{yx}^D & 0 \end{bmatrix} = \begin{bmatrix} 0 & D_{xy}^Z \\ D_{yx}^Z & 0 \end{bmatrix} \begin{bmatrix} 0 & Z_{xy}^U \\ Z_{yx}^U & 0 \end{bmatrix} \quad (7)$$

117 and

$$118 \quad \begin{bmatrix} 0 & Z_{xy}^t \\ Z_{yx}^t & 0 \end{bmatrix} = \begin{bmatrix} 0 & D_{xy}^Z \\ D_{yx}^Z & 0 \end{bmatrix} \begin{bmatrix} 0 & Z_{xy}^h \\ Z_{yx}^h & 0 \end{bmatrix} \quad (8)$$

119 So

$$120 \quad \begin{bmatrix} 0 & D_{xy}^Z \\ D_{yx}^Z & 0 \end{bmatrix} = \begin{bmatrix} 0 & Z_{xy}^t \\ Z_{yx}^t & 0 \end{bmatrix} \begin{bmatrix} 0 & Z_{xy}^h \\ Z_{yx}^h & 0 \end{bmatrix}^{-1} \quad (9)$$

$$121 \quad \begin{bmatrix} 0 & D_{xy}^Z \\ D_{yx}^Z & 0 \end{bmatrix} = \begin{bmatrix} (Z_{xy}^t)/(Z_{xy}^h) & 0 \\ 0 & (-Z_{yx}^t)/(Z_{yx}^h) \end{bmatrix} \quad (10)$$

122 Substituting equation (10) in equation (7)

$$123 \quad \begin{bmatrix} 0 & Z_{xy}^D \\ Z_{yx}^D & 0 \end{bmatrix} = \begin{bmatrix} (Z_{xy}^t)/(Z_{xy}^h) & 0 \\ 0 & (-Z_{yx}^t)/(Z_{yx}^h) \end{bmatrix} \begin{bmatrix} 0 & Z_{xy}^U \\ Z_{yx}^U & 0 \end{bmatrix} \quad (11)$$

124 The undistorted or corrected impedance tensor component can be obtained as

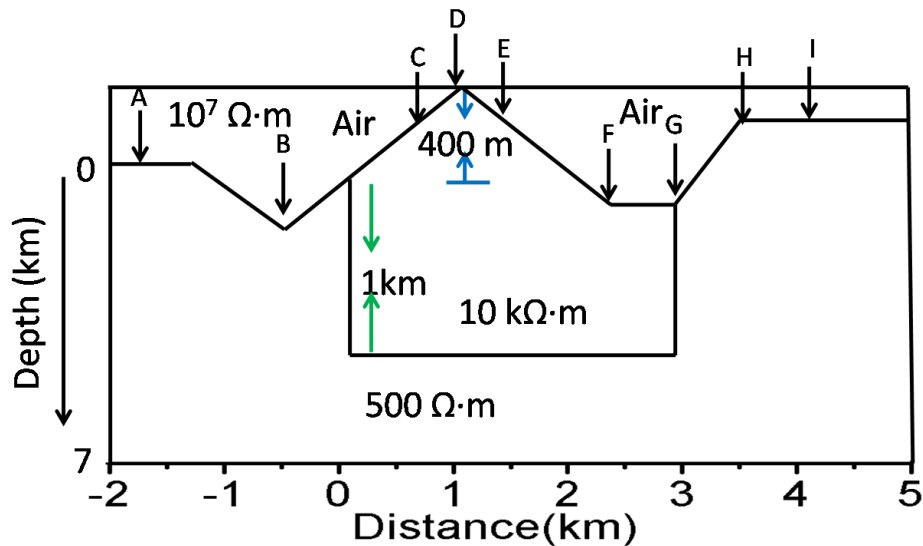
125 So

$$126 \quad Z_{xy}^U = (Z_{xy}^h Z_{xy}^D)/(Z_{xy}^t) \quad (12)$$

$$127 \quad Z_{yx}^U = (Z_{yx}^h Z_{yx}^D)/(Z_{yx}^t) \quad (13)$$

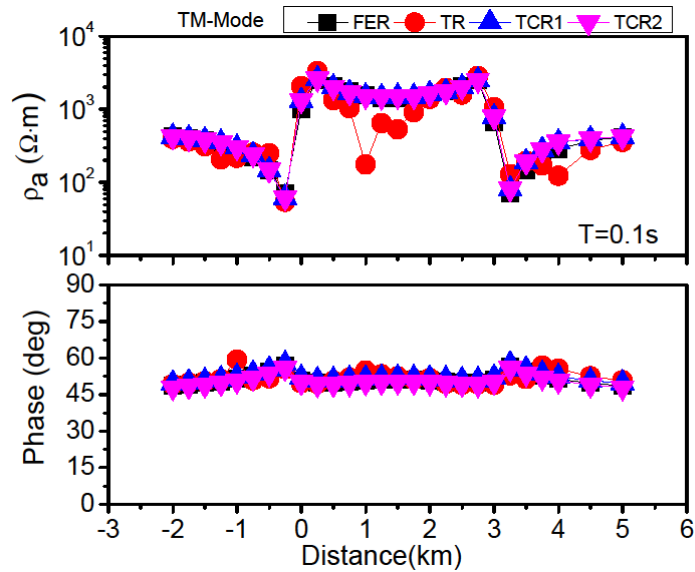
128 **3. TESTING THE CORRECTION PROCEDURES:**

129 In this study, we replicated the model of Chouteau and Bouchard (1988). A 2D topographic  
 130 homogeneous model of  $500 \Omega\cdot\text{m}$  half-space with a resistive block of  $10 \text{ k}\Omega\cdot\text{m}$  having a thickness of 1  
 131 km was embedded in the model from surface relief (Figure 1). The MT responses for the model have  
 132 been computed with and without topography. The terrain correction procedures (TCP1 & TCP2) have  
 133 been applied to the model responses at a particular period of 0.1 second (sec) and validated over the  
 134 inhomogeneous model of Chouteau and Bouchard (1988). The two topography corrected responses  
 135 were analysed at nine different sites (denoted by A, B, C, D, E, F, G, H & I) as shown in Figure 1 at six  
 136 distinct time periods (0.001 sec, 0.01 sec, 0.1 sec, 1 sec, 10 sec, and 100 sec). In 2D the topography  
 137 effect is galvanic in TM mode and inductive in TE mode. Therefore, the comparison of TM  
 138 component of flat earth response (FER), topographic response (TR) and two terrain correction  
 139 responses (TCR1 and TCR2) were shown in Figure 2. It is concluded from the Figure 2 that the TCR1  
 140 and TCR2 are very similar to the FER at particular period of 0.1 sec, but not similar to the TR, which  
 141 shows a good agreement of published result of Chouteau and Bouchard (1988).



142

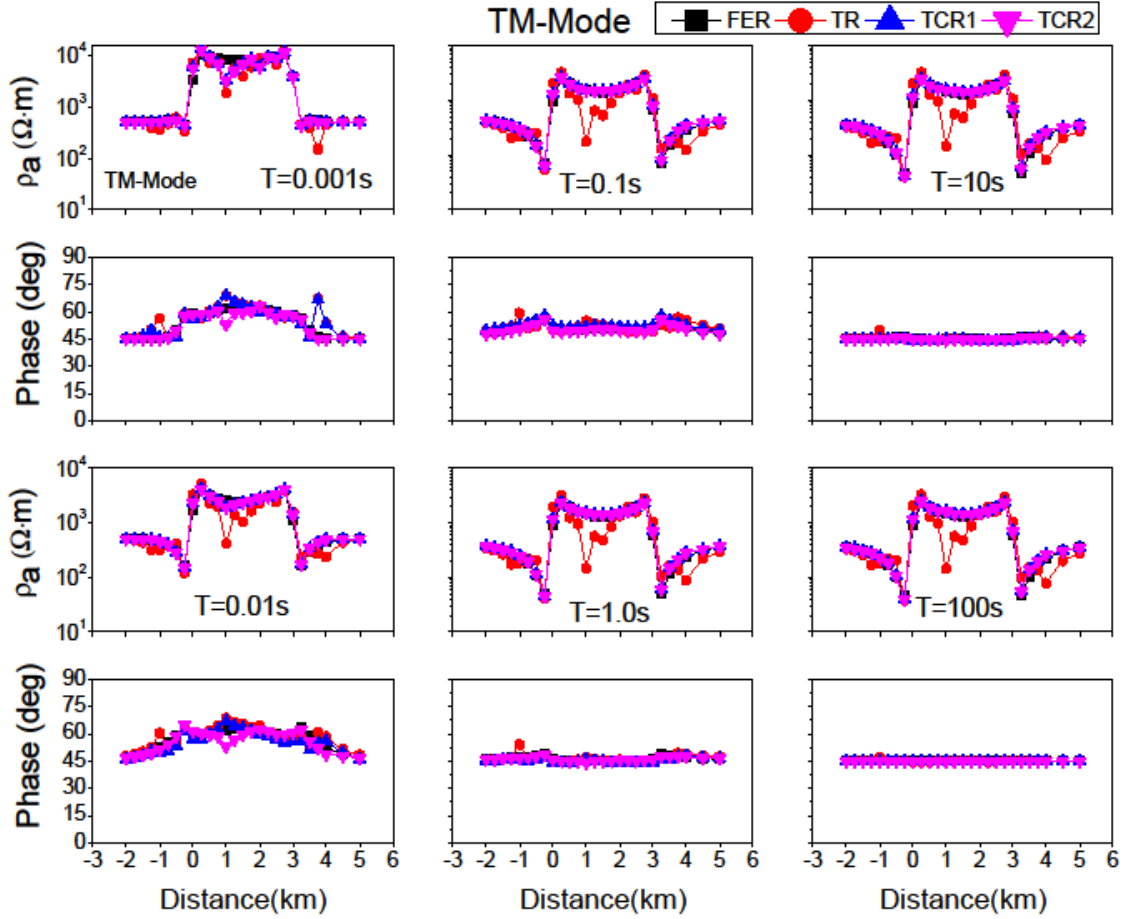
143 **Figure1:** Topographic model of  $500 \Omega\cdot\text{m}$  half-space with a resistive body of  $10 \text{ k}\Omega\cdot\text{m}$  was embedded  
144 from the surface relief (Chouteau and Bouchard, 1988).



145  
146 **Figure2:** Comparison of TM component of flat earth response (FER), topographic response (TR) and  
147 two terrain correction responses (TCR1 and TCR2) at 0.1 sec.

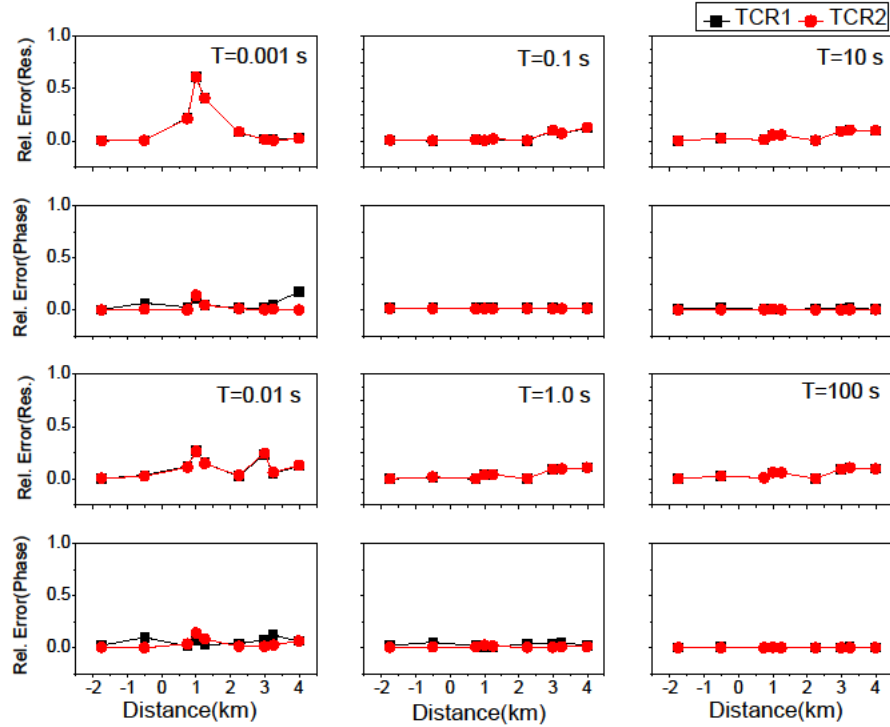
148 Figure3 showed that the topography distortions are large for higher period in apparent resistivity  
149 component only, which shows the galvanic nature of the topography distortions. The terrain corrected  
150 responses (TCR1 and TCR2) in Figure 3 are almost similar to flat earth responses (FER) at six periods  
151 (0.001 sec, 0.01 sec, 0.1 sec, 1 sec, 10 sec, and 100 sec respectively). Relative errors were also  
152 calculated to check the accuracy of the terrain correction responses (TCR1 and TCR2) with flat earth  
153 responses at these periods. The relative error between the FER and TCR1 and TCR2 were very small  
154 at all these periods except at site D only at lower periods (because of  $10 \text{ k}\Omega\cdot\text{m}$  resistive body) as  
155 shown in Figure4. This shows the accuracy of the correction procedures.





156

157 **Figure3:** Comparison of TM components of flat earth response (FER), topographic response (TR),  
 158 and two correction procedures (TCR1 and TCR2) for the model in Figure 1 at six different periods  
 159 (0.001 sec, 0.01 sec, 0.1 sec, 1sec, 10 sec and 100 sec).

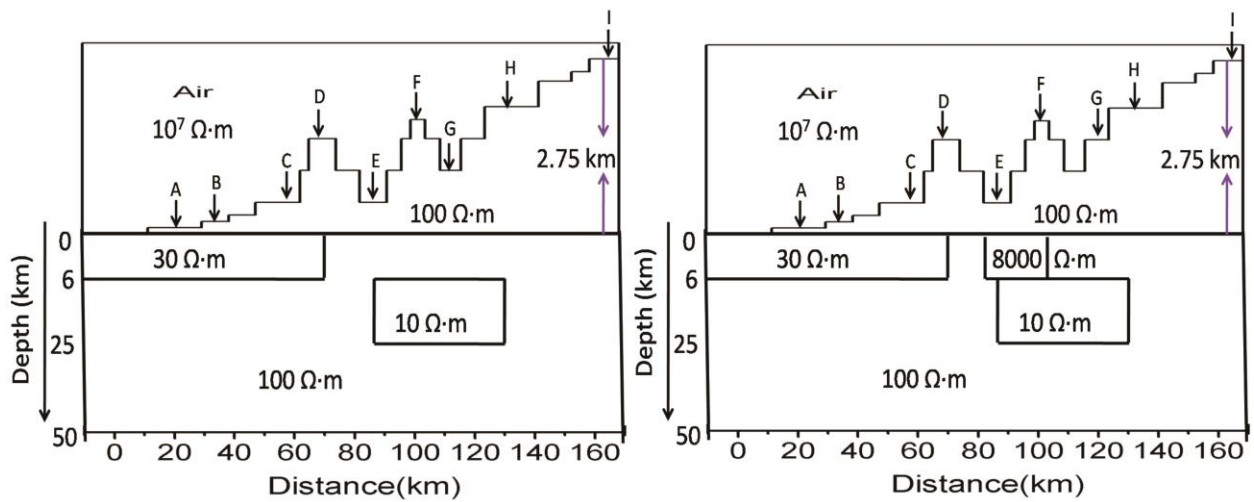


160  
 161 **Figure4:** Relative error between terrains corrected responses (TCR1 and TCR2) with respect to flat  
 162 earth responses (apparent resistivity and phase) at six different periods with homogeneous half-space  
 163 of 500  $\Omega \cdot m$  resistivity.

164 **4. MODELING OF ROORKEE TO GANGOTRI SECTION:**

165 A theoretical analysis of the effect of topography on MT responses was also taken into account in the  
 166 Himalayan topography model. A theoretical model of Roorkee-Gangotri Profile was generated to  
 167 simulate the MT response. To compute the MT forward modeling responses over the rugged  
 168 topographic surface in Roorkee to Gangotri section, the input model was prepared from a 2D inverted  
 169 geoelectrical resistivity model (Tyagi, 2007). The topography model having an elevation of 2.75 km  
 170 consists of a 180 km long profile from Roorkee to Gangotri drawn (Tyagi, 2007; Suman et al., 2023).  
 171 In this model, two conductive blocks having resistivity 30  $\Omega \cdot m$  and 10  $\Omega \cdot m$  were embedded in a  
 172 homogeneous half-space of 100  $\Omega \cdot m$  resistivity. The first block of resistivity 30  $\Omega \cdot m$  having width 80

173 km and thickness 6 km was embedded just near the earth's surface relief and the second block of width  
 174 40 km and thickness 25 km was embedded at 6 km depth from the surface. The MT responses were  
 175 computed by considering three models, (1) one with half-space of resistivity  $100 \Omega\cdot\text{m}$  (Figure5a), (2)  
 176 with half-space of resistivity  $500 \Omega\cdot\text{m}$ , (3) with an additional resistive body of  $8000 \Omega\cdot\text{m}$  embedded  
 177 from earth surface relief having thickness about 6 km with half-space of resistivity  $100 \Omega\cdot\text{m}$  as shown  
 178 in Figure5b. The topography response (TR), flat earth response (FER) and two topography corrected  
 179 responses (TCR1 & TCR2) were analysed for nine sites (A, B, C, D, E, F, G, H & I) as shown in  
 180 Figure5 at six distinct periods (0.0013 sec, 0.0102 sec, 0.1063 sec, 1.1110 sec, 11.6078 sec, and  
 181 121.2813 sec).



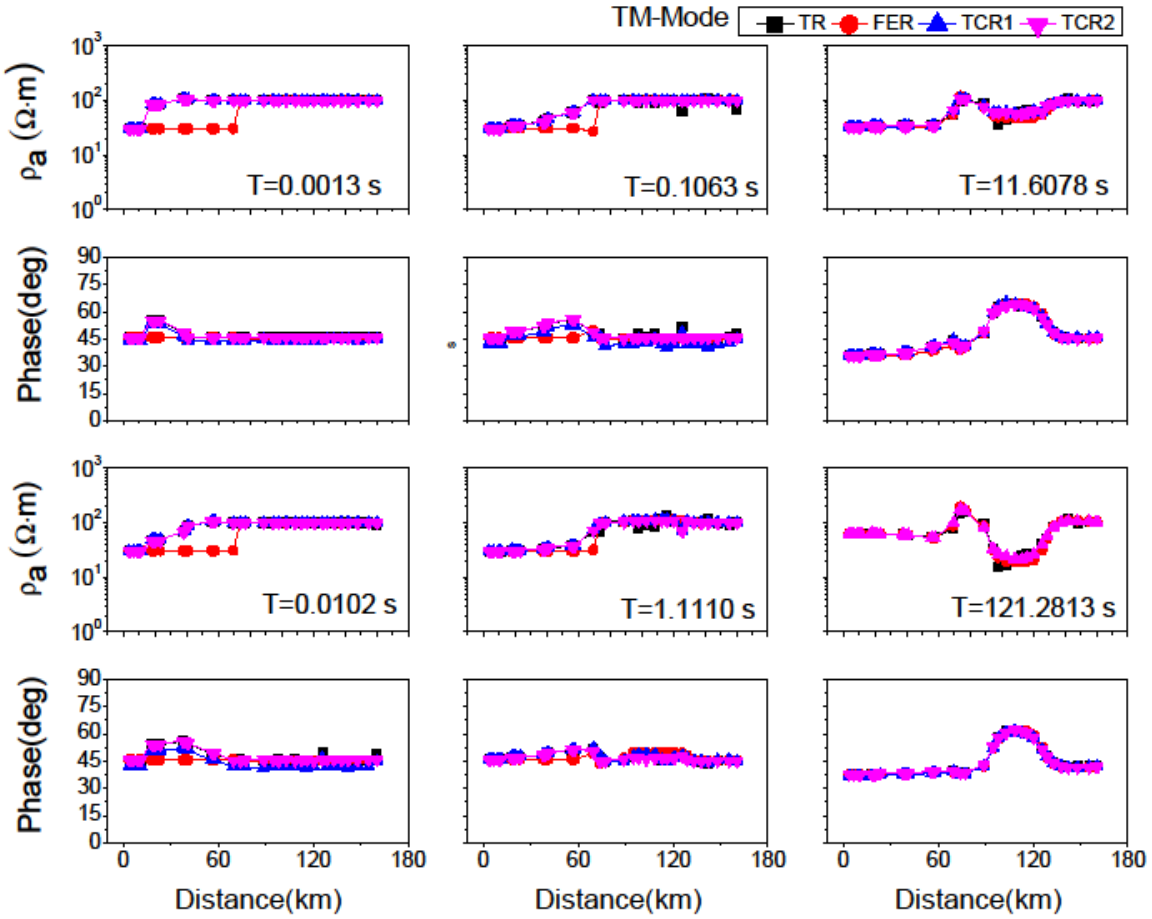
182  
 183 **Figure5:** (a) A Synthetic model of Garhwal Himalaya along Roorkee to Gangotri Profile in half-space  
 184 of resistivity  $100 \Omega\cdot\text{m}$  (b) with a resistive block of resistivity  $8000 \Omega\cdot\text{m}$ .

185 **5. RESULT AND DISCUSSION:**

186 **5.1. Model with half-space of resistivity  $100 \Omega\cdot\text{m}$ :**

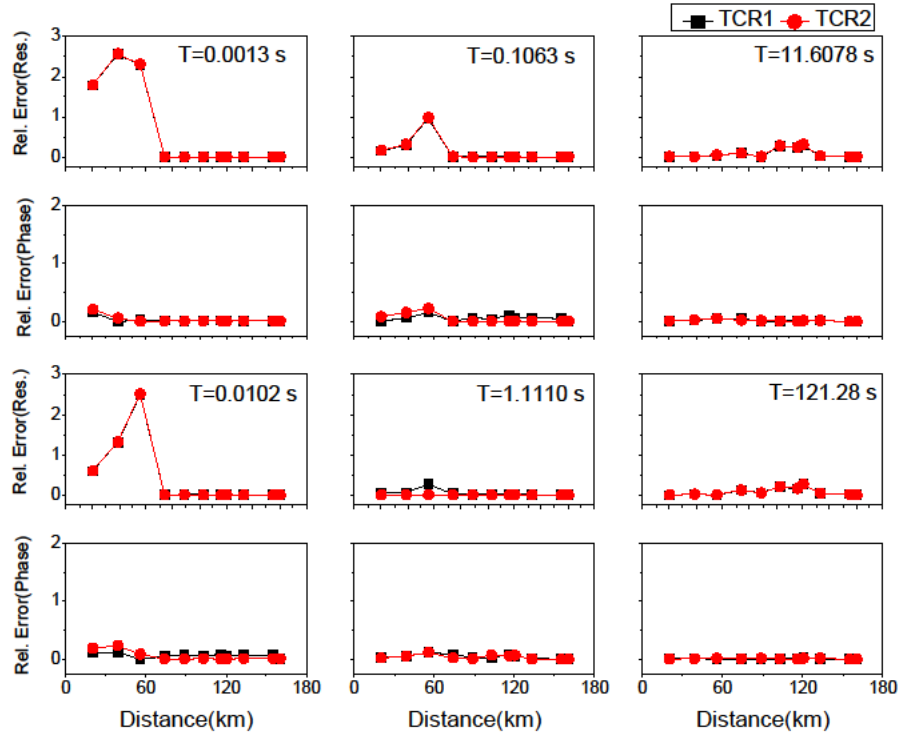
187 The topography response (TR) and flat earth response (FER) were computed for the topography  
 188 model with a conductive body of  $30 \Omega\cdot\text{m}$  resistivity in a half-space of  $100 \Omega\cdot\text{m}$  resistivity (Figure

189 5a) and the topography corrections procedures were applied to the MT data. Figure 6 shows the TM  
190 mode of topography response (TR), flat earth response (FER) and two topography correction  
191 responses (TCR1 & TCR2) at six different periods (0.0013 sec, 0.0102 sec, 0.1063 sec, 1.1110 sec,  
192 11.6078 sec, and 121.2813 sec). The topography effect depends upon the ramp/slope angle of the hill  
193 and is significant when the slope angle is greater than  $7.5^\circ$  (Kumar et al., 2018). It is clear from  
194 Figure 6 that the TCR1 and TCR2 are almost similar to the topographic response, because the slope  
195 angle is less than  $1^\circ$ . The TCR1 & TCR2 were not similar to the flat earth response for the sites from A  
196 to D at lower periods 0.0013 sec, 0.0102 sec, 0.1063 sec and 1.1110 sec, because of the exposure of  
197 the conductive body having resistivity  $30 \Omega \cdot m$  to the surface (from A to D) and its galvanic effect. The  
198 relative errors were also calculated between the FER with TCR1 and TCR2 and were high for the sites  
199 A, B and C for lower periods (0.0013 sec, 0.0102 sec and 0.1063 sec) due to the presence of the  
200 conductive body underneath these sites and was very small for all other sites D, E, F, G, H and I at all  
201 periods as shown in Figure 7.



202

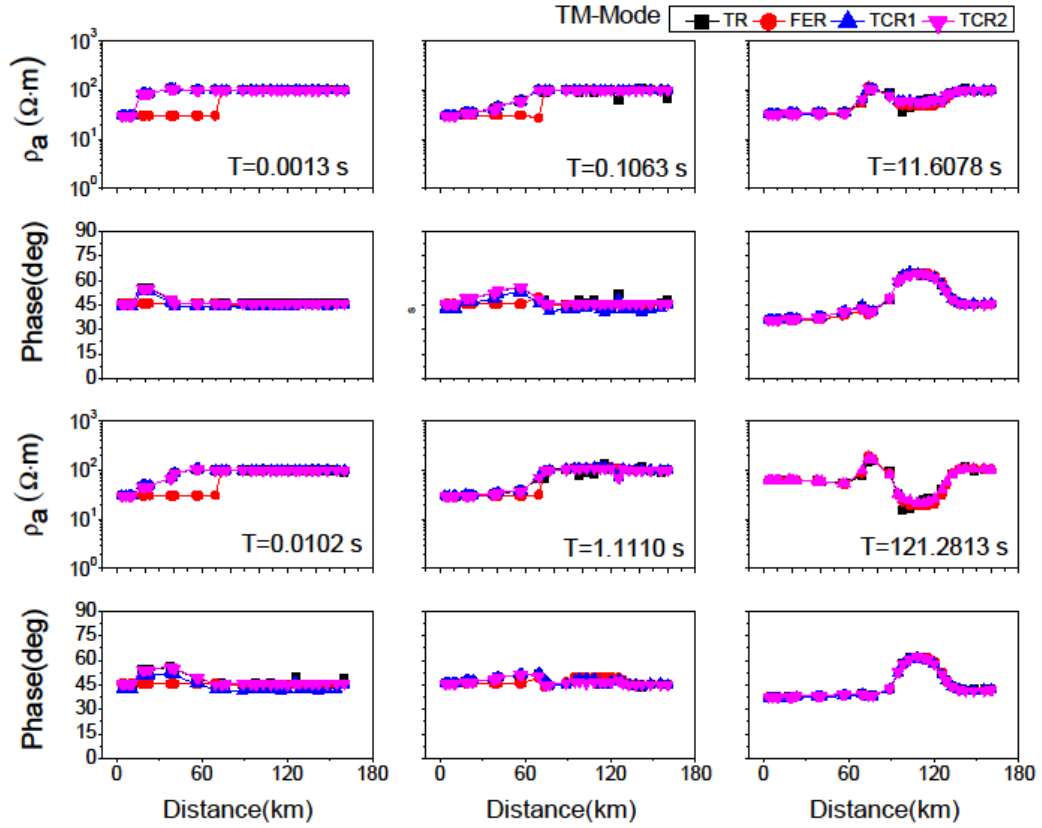
203 **Figure6:** Comparison of TM components of flat earth response (FER), topographic response (TR),  
 204 and two correction procedures (TCR1 and TCR2) at six different periods for homogeneous half-space  
 205 of resistivity  $100 \Omega \cdot m$ .



206  
 207 **Figure 7:** Relative error between terrains corrected responses (TCR1 and TCR2) with respect to flat  
 208 earth response (apparent resistivity and phase) at six different periods with half-space of resistivity  
 209 100  $\Omega\cdot\text{m}$ .

210 **5.2. Model with half-space of resistivity 500  $\Omega\cdot\text{m}$ :**

211 Now consider the case in which model half-space resistivity was replaced with 500  $\Omega\cdot\text{m}$  in Figure 5a.  
 212 The topography response (TR) and flat earth response (FER) were computed for the topography  
 213 model with half-space of 500  $\Omega\cdot\text{m}$  resistivity (Figure 5a) and the topography correction procedures  
 214 were applied to the MT data. Figure 8 shows the TM component of topography response (TR), flat  
 215 earth response (FER), and topography corrected responses (TCR1 & TCR 2) at six different periods.  
 216 The results were almost similar to the response of the model with half-space of resistivity 100  $\Omega\cdot\text{m}$ .  
 217 The relative errors were also calculated in this case also between the FER with TCR1 and TCR2 and  
 218 the results were similar to the model with half-space of 100  $\Omega\cdot\text{m}$  at all these periods (0.0013 sec,  
 219 0.0102 sec, 0.1063 sec, 1.1110 sec, 11.6078 sec, and 121.2813 sec) as shown in Figure 9.

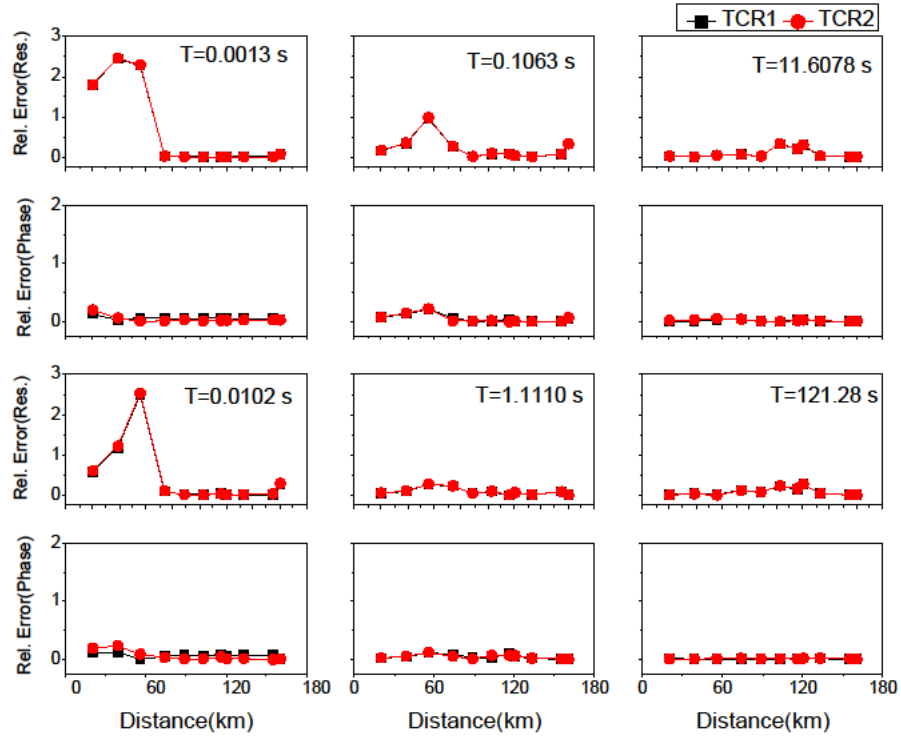


220

221 **Figure8:** Comparison of TM components of flat earth response (FER), topographic response (TR),

222 and two correction procedures (TCR1 and TCR2) at six different periods for half-space of resistivity

223 500  $\Omega \cdot m$ .



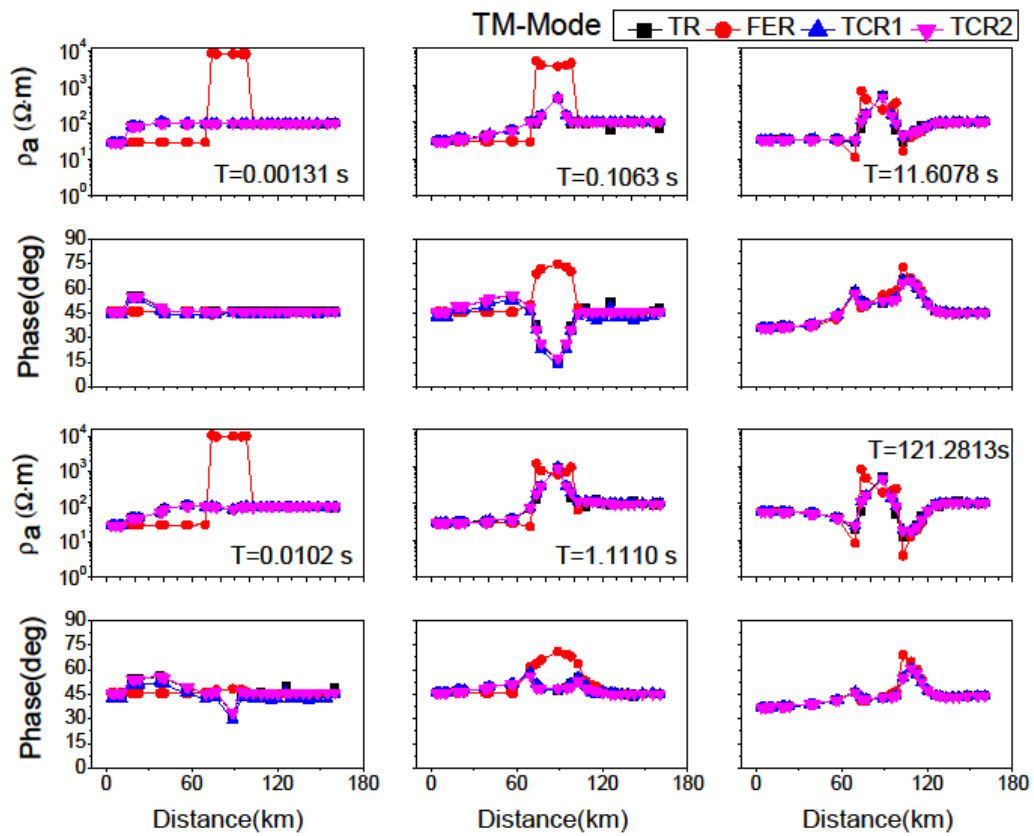
224  
 225 **Figure9:** Relative error between terrains corrected responses (TCR1 and TCR2) with respect to flat  
 226 earth response (apparent resistivity and phase) at six different periods with half-space of resistivity  
 227 500  $\Omega \cdot m$ .

228 **5.3. Model with a resistive block of resistivity 8000  $\Omega \cdot m$  in half-space of 100  $\Omega \cdot m$ :**

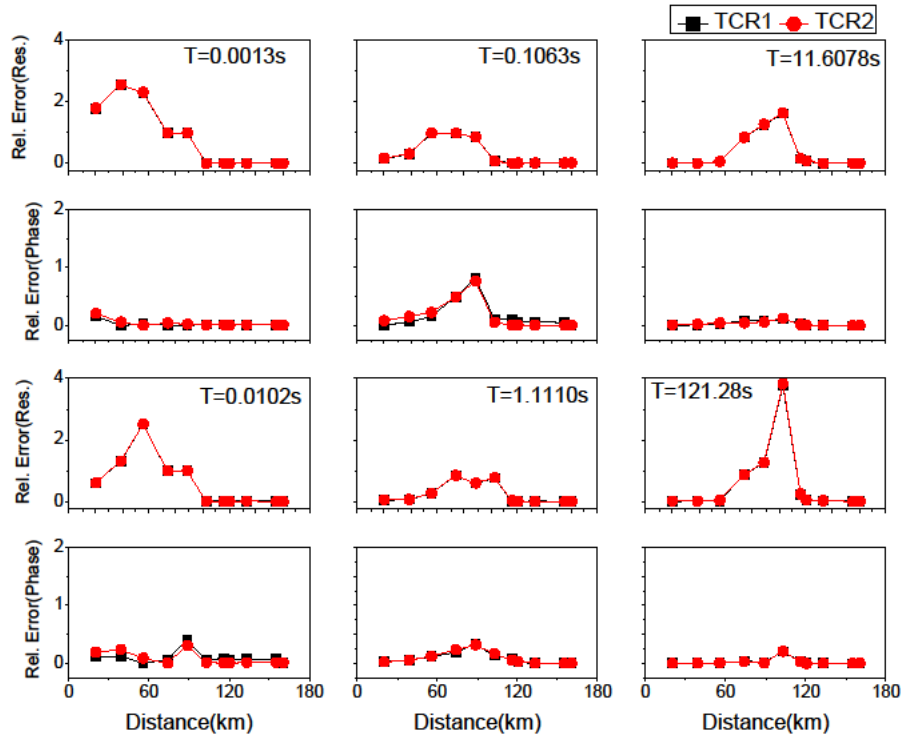
229 The topography response (TR) and flat earth response (FER) were also computed for the topography  
 230 model with a resistive block of resistivity 8000  $\Omega \cdot m$  in half-space of 100  $\Omega \cdot m$  resistivity (Figure 5b)  
 231 and the topography corrections were applied to the MT data. Figure10 shows the TM component of  
 232 topography response (TR), flat earth response (FER) and two topography correction responses (TCR1  
 233 & TCR2) at six different periods. The TCR1 & TCR2 were not similar to the flat earth model for the  
 234 sites from A to F, because of the exposure of the conductive body having resistivity 30  $\Omega \cdot m$  to the  
 235 surface (from A to D) and its galvanic effect and the presence of 8000  $\Omega \cdot m$  resistive body (from D to



236 F). The relative errors were also calculated between the FER with TCR1 and TCR2 and were high for  
 237 the sites A, B and C for lower periods (0.0013 sec, 0.0102 sec and 0.1063 sec) due to the presence of  
 238 the conductive body underneath these sites and for higher periods (1.1110 sec, 11.6078 sec and  
 239 121.2813 sec) the relative error was again high due the presence of the 8000  $\Omega\cdot m$  resistive body from  
 240 D to F as shown in Figure 11.



241  
 242 **Figure10:** Comparison of TM components of flat earth response (FER), topographic response (TR),  
 243 and two correction procedures (TCR1 and TCR2) at six different periods for half-space of resistivity  
 244 100  $\Omega\cdot m$ .



245

246 **Figure11:** Relative error between terrains corrected responses (TCR1 and TCR2) with respect to flat  
 247 earth response (apparent resistivity and phase) at six different periods with half-space of resistivity  
 248 100  $\Omega \cdot m$ .

249 **6. CONCLUSIONS:**

250 The study shows the effect of topography in the MT data along a synthetic model of Roorkee-  
 251 Gangotri profile. The two correction procedures were used to remove the topography distortion from  
 252 MT data. The similar FER, TCR1 and TCR2 in Figure. 3 shows that the both correction procedures  
 253 are capable to remove the topography effect, this shows the accuracy of the two correction procedures.  
 254 The similar TR, TCR1 and TCR2 responses (Figure 6, 8 and 10) concluded that there is no need for  
 255 topography correction along Roorkee-Gangotri Profile, because the slope angle is less than one  
 256 degree. The relative error between the FER and TCR1 and TCR2 also showed the accuracy of the two

257 correction procedures (TCR1 & TCR2) in this study. The presence of near surface  
258 heterogeneity/surface exposure of conductive/resistive body also distort the MT responses as in this  
259 model (the FER not similar to TR, TCR1 and TCR2).

## 260 **ACKNOWLEDGEMENT**

261 S. Saini thank Head of Department, Department of Physics, M. M. Engineering College, Maharishi  
262 Markandeshwar (Deemed to be) University for continuous guidance and support throughout this  
263 research.

## 264 **AUTHOR CONTRIBUTION:**

265 Dr. Deepak Kumar Tyagi and MsSumanSaini designed the experiments, developed the model  
266 and performed the simulations. Dr Rajeev Sehrawat, Dr. Sushil Kumar prepared the manuscript  
267 with contributions from all the co-authors.

## 268 **COMPETING INTERESTS**

269 The authors declare that they have no conflict of interest.

## 270 **REFERENCES**

- 271 1. Cagniard, L.: Basic theory of the magneto-telluric method of geophysical prospecting.  
272 Geophysics. **18** 605-635, 1953.
- 273 2. Changhong, Lin.: The effects of 3D topography on controlled-source audio-frequency  
274 magnetotelluric responses. Geophysics. **83** no. 2 p. Wb97–wb108, 1910.1190/geo-0429, 2018.
- 275 3. Chouteau, M., and Bouchard, K.: Two-dimensional terrain correction in magnetotelluric **Surveys**.  
276 Geophysics. **53** 854-862, 1988.

- 277 4. Coggon, H.: Electromagnetic and electrical modeling by the finite-element method: *Geophysics*.  
278 **36** 132-155, 1971.
- 279 5. Faradzhev, A. S., Kakhramanov, K. K., Sarkisov, G. A., and Khalilova, N. E.: On effects of  
280 terrain on magnetotelluric sounding (MTS) and profiling (MTP). *Izvestia Earth Physics*. **5** 329-  
281 330, 1972.
- 282 6. Franke, A., Börner, R. U., and Spitzer, K.: Adaptive unstructured grid finite element simulation of  
283 two-dimensional magnetotelluric fields for arbitrary surface and seafloor topography.  
284 *Geophysical Journal International*. **171** 71-86, 2007.
- 285 7. Gurer, A., and Ilkisik, M.: The importance of topographic corrections on magnetotelluric response  
286 data from rugged regions of Anatolia, *Geophys. Prospect*. **45** 111-125, 1997.
- 287 8. Harinarayana, T., and Sarma, S. V. S.: Topographic effects on telluric field measurements.  
288 *Pageoph*. **120** 778-783, 1982.
- 289 9. Holcombe, H. T., and Jiracek, G. R.: 1984 Three-dimensional terrain corrections in resistivity  
290 surveys: *Geophysics*. **49** 439-452, 1977.
- 291 10. Israil, M., Tyagi, D. K., Gupta, P. K., and Niwas, Sri.: Magnetotelluric investigations for imaging  
292 electrical structure of Garhwal Himalaya corridor, Uttarakhand, India. *Journal of Earth System*  
293 *Sci.* **117** 189-200, 2008.
- 294 11. Israil, M., Mamoriya, P., Gupta, P. K., and Varshney, S. K.: Transverse Tectonics Feature  
295 Delineated by Modelling of Magnetotelluric Data from Garhwal Himalaya Corridor, India. *Curr.*  
296 *Sci.* **111** 868-875, 2016.
- 297 12. Jiracek, G. R., Redding, R. P., and Kojima, R. K.: Application of the Rayleigh-FFT  
298 technique to magnetotelluric modeling and correction. *Physics of the Earth and Planetary*  
299 *Interiors*, **53** 365-375, 1989.
- 300 13. Jiracek, G.: Near-surface and topographic distortions in electromagnetic induction. *Surveys*  
301 *Geophysics*. **11** 163-203, 1990.
- 302 14. Konda, S., Patro, P. K., Reddy, K. C., and Babu, N.: Three-dimensional magnetotelluric  
303 signatures and rheology of subducting continental crust: Insights from Sikkim Himalaya, India.  
304 *Journal of Geodynamics*. **155** 101961, 2023.
- 305 15. Ku, C. C., Hsieh, M. S., and Lim, S. H.: The topographic effect in electromagnetic fields. *Can. J.*  
306 *Earth Sci.* **10** 645-656, 1973.

- 307 16. Kumar, D., Singh, A., and Israil, M.: Necessity of Terrain Correction in Magnetotelluric Data  
308 Recorded from Garhwal Himalayan Region, India. *Geosciences*. **11** 482, 2021.
- 309 17. Kumar, G. P., Manglik, A., and Thiagarajan, S.: Crustal Geoelectric Structure of the Sikkim  
310 Himalaya and Adjoining Gangetic Foreland Basin. *Tech. physics*. **637** 238-250, 2014.
- 311 18. Kumar, S., Patro, P. K., and Chaudhary, B. S.: Three dimensional topography correction applied  
312 to magnetotelluric data from Sikkim Himalayas. *Physics Earth Planet. Int.* **279** 33-46, 2018.
- 313 19. Kumar, S., Patro, K. P., and Chaudhary, B. S.: Subsurface Resistivity Image of Sikkim Himalaya  
314 as Derived from Topography Corrected Magnetotelluric Data. *Journal of the Geological Society  
315 of India*. DOI: 10.1007/s12594-022-1985-2, 2022.
- 316 20. Kunetz G. and DeGery J. C.: Exemples d'application de la representation conform  
317 al'interpretation du champ tellurique. *Revue De L'institut Franc ais Du Pe'trole* 11, 1179-1192,  
318 1956.
- 319 21. Larsen, J. C.: Removal of local surface conductivity effects from low frequency mantle response  
320 curves, *Acta Geodaet., Geophys. et Montanist. Acad. Sci. Hung. Tomus.* **12** (1-3) 183-186, 1977.
- 321 22. Mohan, K., Kumar, G. P., Chaudhary, P., Choudhary, V. K., Nagar, M., Khuswaha, D., Patel, P.,  
322 Gandhi, D., and Rastogi, B. K.: Magnetotelluric Investigations to Identify Geothermal Source  
323 Zone near Chabsar Hotwater Spring Site, Ahmedabad, Gujarat, Northwest India. *Geothermics*.  
324 **65** 198-209, 2017.
- 325 23. Nam, M. J., Kim, H. J., Song, Y., Lee, T. J., Son, J. S., and Suh, J. H.: Three-dimensional  
326 topography corrections of magnetotelluric data. *Geophysics J. Int.* **174** 464-474, 2008.
- 327 24. Ngoc, P. V.: Magnetotelluric survey of the Mount Meager region of the Squamish Valley (British  
328 Columbia). *Geomagnetic Service of Canada, Earth Physics Branch of the Dept. of Energy,  
329 Mines and Resources of Canada. Rep.* 80-8-E, 1980.
- 330 25. Patro, P. K., and Harinarayana, T.: Deep Geoelectric Structure of the Sikkim Himalayas (NE  
331 India) Using Magnetotelluric Studies. *Phys. Earth Planet. Inter.* **173** 171-176, 2009.
- 332 26. Patro, P. K.: Magnetotelluric Studies for Hydrocarbon and Geothermal Resources: Examples  
333 from the Asian Region. *Surveys Geophysics*. **38** 1005-1041, 2017.
- 334 27. Pek, J and Verner, T.: Finite-difference modelling of magnetotelluric fields in two-dimensional  
335 anisotropic media. *Geophys. J. Int.* **128**, 505-521, 1997.
- 336 28. Rastogi, A.: A finite difference algorithm for two-dimensional inversion of geo-  
337 electromagnetic data. Ph. D. Thesis, University of Roorkee (India), 1997.

- 338 29. Redding, R. P. and Jiracek, G. R.: Topographic modeling and correction in magnetotellurics. In  
339 54th Annual International Meeting, Society of Exploration Geophysicists, Expanded Abstract.  
340 44-47, 1984
- 341 30. Rijo, L.: Modelling of electric and electromagnetic data: Ph.D. thesis, Univ. of Utah. **19**, 1977.
- 342 31. Suman, Tyagi, D. K., and Sherawat, R.: Topography distortion effect on Magnetotelluric (MT)  
343 profiling of Sub-Himalayan region using two-dimensional modelling. *J. Integr. Sci. Technol.* **11**  
344 462, 2023.
- 345 32. Thayer, R.E.: Topographic distortion of telluric currents: a simple calculation. *Geophysics.* **40** 91-  
346 95, 1975.
- 347 33. Tikhonov, A. N.: Determination of the Electrical Characteristics of the Deep Strata of the Earth's  
348 Crust. *DoklAkadamiyaNauk.* **73** 295-297, 1950.
- 349 34. Tyagi, D. K.: 2D modeling and inversion of magnetotelluric data acquired in Garhwal Himalaya,  
350 Ph. D. Thesis, 2007.
- 351 35. Vozoff, K.: The magnetotelluric method, in *Electromagnetic Methods in Applied Geophysics*.ed.  
352 Nabighian, M. N., Society of Exploration Geophysicists. **2** 641-711, 1991.
- 353 36. Wannamaker, P. E., Stodt, J. A., Rijo, L.: Two-dimensional topographic responses in  
354 magnetotellurics modeled using finite elements. *Geophysics.* **51** 2131-2144, 1986.
- 355 37. Ward, S. H., Peeples, W. J., and Ryu, J.: Analysis of geo-electromagnetic data: *Meth. Compo*  
356 *Phys.* **13** 163-238, 1973.
- 357 38. Wescott, E. M., and Hessler, V. P.: The effect of topography and geology on telluric currents.  
358 *Jour. Geophysics. Res.* **67** 4813-4823, 1962.
- 359 39. Xiong, B., Luo, T. Y., Chen, L. W., Dai, S. K., Xu, Z. F., Li, C. W., Ding, Y. L., Wang, H. H.,  
360 and Li, J. H.: Influence of Complex Topography on Magnetotelluric Observed Data Using  
361 Three-Dimensional Numerical Simulation: A Case from Guangxi Area, China. *Appl.*  
362 *Geophysics.* **17** 601-615, 2020.
- 363 40. Yutaka Sasaki.: 3-D electromagnetic modelling and inversion incorporating topography. ASEG  
364 Extended Abstracts, 2003:1, 1-7, DOI: 10.1071/ ASEG2003\_3DEMab013, 2003
- 365 41. Zhang, K., Wei, W., Lu, Q., Dong, H., and Li, Y.: Theoretical Assessment of 3-D Magnetotelluric  
366 Method for Oil and Gas Exploration: Synthetic Examples. *J. Appl. Geophysics.* **106** 23-36,  
367 2014.

368

